

A Proposed Methodology for Magnetic Resonance Images' Geometrical Distortion Correction Intended To Use For Radiotherapy Planning Using a Large Inhouse Field of View

Atefeh Rostami^{1*}, Shahrokh Naseri², Mahdi Momenzad³, Hoda Zare², Kazem Anvari⁴, Hamed Reza Sayah Badkhor⁵, Vajiheh Vajdani Noghreiyani¹

1. Department of Medical Physics and Radiological Sciences, Sabzevar University of Medical Sciences, Sabzevar, Iran
2. Medical Physics Research Center, Mashhad University of Medical Sciences, Mashhad, Iran
3. Nuclear Medicine Research Center, Mashhad University of Medical Sciences, Mashhad, Iran
4. Department of Radiotherapy Oncology and Cancer Research Center, Mashhad University of Medical Sciences, Mashhad, Iran
5. Kowsar MRI Center, Emam Reza Hospital, Mashhad, Iran

ARTICLE INFO	ABSTRACT
<p>Article type: Original Paper</p> <hr/> <p>Article history: Received: Feb 08, 2022 Accepted: Aug 05, 2021</p> <hr/> <p>Keywords: Geometrical Distortion Spatial Distortion Correction 3D Slicer Scatter Transform B-Spline Deformable Registration</p>	<p>Introduction: Exquisite soft tissue contrast of magnetic resonance images (MRI) and the new combined radiotherapy system of MR-Linac have been the main impetus for applying MR imaging in radiotherapy. One limitation of MR-based radiotherapy is the geometric distortion of MR images that can generate errors in the contouring and dosimetry stages. This study aimed to evaluate and correct geometric distortion for radiotherapy applications.</p> <p>Material and Methods: A large field of view (FOV) phantom develop using Perspex sheets and 325 plastic pipes. The quantification and correction of MR images' system-related geometric distortion are conducted for HASTE protocol by MATLAB and 3D slicer software in phantom and patient images. The effect of MRI images geometrical distortion was evaluated for ten patients undergoing body radiotherapy treatment. CT images were used as a primary dataset to estimate the distortion map.</p> <p>Results: The phantom investigation results indicate that in radial distances of < 13 cm (or FOVs < 25 cm), the amount of distortion is under 2 mm. Still, at more considerable radial distances, distortion may increase up to about 3.5 cm. MR images of Patients with lateral (LAT) and anterior-posterior (AP) diameters of more than 38 cm and 25 cm respectively, need to be corrected for geometric distortion.</p> <p>Conclusion: MR images' geometric precision in large FOVs is not sufficient for MRI only treatment planning of radiotherapy and further corrections are required. The B-spline deformable registration method can correct the MR geometric distortion until an acceptable range of 2 mm for radiotherapy applications.</p>

► Please cite this article as:

Rostami A, Naseri Sh, Momenzad M, Zare H, Anvari K, Sayah Badkhor HR, Vajdani Noghreiyani V. A Proposed Methodology for Magnetic Resonance Images' Geometrical Distortion Correction Intended To Use For Radiotherapy Planning Using a Large Inhouse Field of View. Iran J Med Phys 2022; 19: 305-314. 10.22038/IJMP.2022.55684.1920.

Introduction

Computed tomography (CT) imaging is the gold standard for radiotherapy treatment planning due to its geometrical precision and the electron density information provided for dose calculation [1]. However, magnetic resonance imaging (MRI) offers exquisite soft tissue contrast compared to CT besides the diversity of imaging protocols and the possibility of functional imaging [2-6]. Given the advantages of MRI imaging, the images of two MRI and CT modalities can be co-registered for radiotherapy treatment planning. That is, MRI images are used for soft tissue contouring and CT images for geometrical accuracy and dose calculations. Nevertheless, there are some uncertainties associated with MRI and CT images fusion that causes errors for the target and organ at risk localization, in addition to the time consuming of MRI/CT image registration and associated costs of the

two imaging modalities, and radiation dose of CT imaging [7, 8]. The new combined MRI-guided linear accelerator (MRI-linac) systems in radiotherapy introduce a new application of MRI imaging for simulation and guided radiotherapy. This machine requires new sets of skills and knowledge regarding MRI and radiotherapy practice [9, 10]. Even recently the American Board of Radiology introduce new sets of subspecialty in "MR in RT" emphasizing more education and patient safety in this area.

MRI-based radiotherapy has four significant drawbacks. 1) MRI images geometric distortion, 2) patient positioning accuracy by choosing the right and MRI compatible device, 3) Accurate radiation dose calculation, and finally, 4) Generate and use of traditional digital radiograph construction (DRR) for patient positioning verification. [11].

One drawback of MR-based simulation is the geometric distortion of MRI images that need to be evaluated and corrected, especially for large patients at large field of views (FOVs) body regions more than 20 cm. [12]. Radiotherapy planning on geometrically distorted MRI images can introduce errors in target and normal tissue delineation and subsequently on the plan quality and patient outcome [7, 8].

Geometrical distortion of MR images can be placed into two categories: a) patient-related distortion, and b) System-related distortion (Figure 1). The patient-related distortion of susceptibility and chemical shift artifacts can be mitigated by the selection of suitable image parameters like the wider receive Bandwidth (rBW) and the adoption of fast spin echo (SE) sequences besides fat saturation techniques [13, 14]. Many studies have shown that the system-related distortions of MR images generated by the magnetic field inhomogeneity and gradient non-linearity are larger than patient-related distortions, especially in modern fast MRI scanners [15, 16]. The system-related distortion can be evaluated using suitable phantoms with adequate markers that are visible in both CT and MR images.

Although each MRI scanner has its correction program algorithms, numerous studies have reported that it is not suitable for radiotherapy applications. MRI images' geometrical distortion must be evaluated and corrected according to the radiotherapy techniques. Several studies have shown distortion is under 2 mm for FOV < 20 cm that is suitable for 3D conformal radiotherapy (CRT), but stereotactic radiosurgery (SRS), stereotactic radiotherapy (SRT), and intensity-modulated radiotherapy (IMRT) techniques need more geometrical precision [16, 17]. Therefore, based on the radiotherapy techniques, suitable and additional correction is required for radiotherapy application. A distortion of more than 2

mm is not acceptable for treatment planning purposes in 3D CRT and it must be evaluated and corrected for each MRI simulator or any MRI machine intended to use for Radiotherapy simulation and planning [17].

The geometric distortion evaluation of MRI images has been done by different designs of 2D and 3D house-made phantoms in several studies [18-25]. Despite the variety of designs used for 2D and 3D phantoms in the geometric distortion assessment of MRI images, few articles have presented a correction method suitable for MR-based treatment planning of radiotherapy in large FOVs. Wang et al. employed grid sheets for the evaluation of geometric distortion, using the piecewise mapping method equipped with the trilinear interpolation for its correction that the maximum reported absolute geometric distortion is 10 mm, which could be reduced to 0.6 mm using the piecewise correction methods [23, 24]. In another study, Price et al. adopted the distortion map as a template to warp distorted images and develop corrected images. The maximum reported distortion is 9.5 mm, which could be reduced to about 1 mm with the correction of geometric distortion [15].

Based on mentioned studies, the geometric distortion of MRI images depends on several parameters including [16, 20, 25]

- Magnetic field strength
- Type of scanner (close or open-bore systems)
- Pulse sequence type (gradient-echo or spin-echo sequences)
- Imaging parameters (TR, TE, and receiver bandwidth)
- Vendor geometric correction algorithm in each scanner (2D or 3D algorithms)

Due to the complication of MRI images geometric distortion and its major effects on contouring and dosimetry, the accurate evaluation of each MRI simulator and each imaging protocol is necessary.

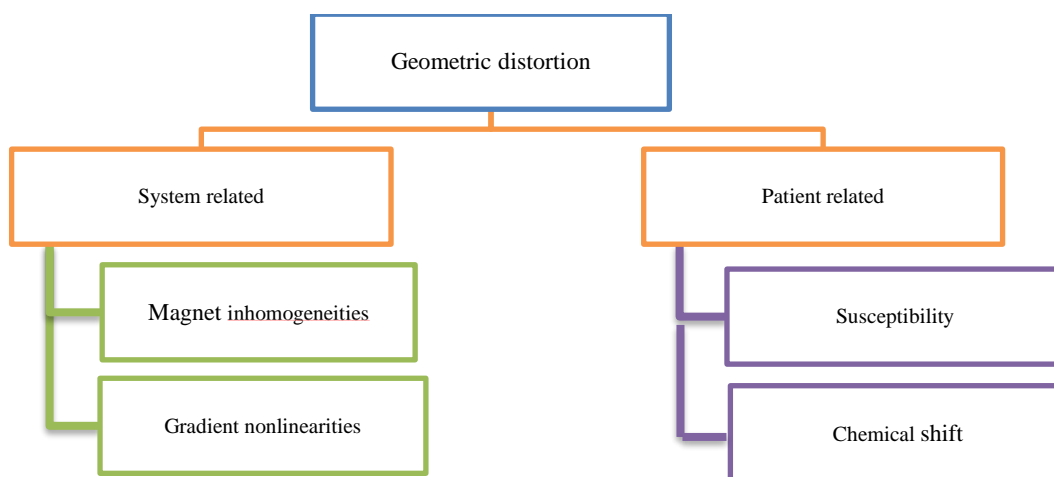


Figure 1. Kinds of Geometrical distortion in MR images

We previously showed the comparison between four MRI images' geometrical correction methods [26]. In this work, we are focusing on the sequence-specific source of MRI image geometrical distortion. We evaluate and correct the system-related geometric distortion of MRI images in the Half-Fourier Acquisition Single-shot Turbo spin Echo (HASTE) MRI imaging pulse sequence used for MRI-based treatment planning in the pelvic region. In this paper, a new 3D large FOV phantom and a novel correction method based on phantom-mapped distortion data are present using the 3D slicer software and B-spline deformable registration method. The function of the correction program is evaluated in phantom and patient images, and the results are discussed.

Materials and Methods

Large FOV phantom

An in-house phantom was developed using 6 Perspex sheets and 325 water pipes as the signal generator for CT and MR imaging to provide a comprehensive mapping of the spatial distortion (Figure 2). In order to evaluate and correct MRI image distortion for MRI-based radiotherapy, a large FOV phantom with dimensions of 48×48×37 cm³ was designed. The details of phantom instruction are reported in our previous study [26] where we compared the amount of distortion in four MR imaging protocols.

CT and MR Imaging of the phantom

CT reference images were captured for the whole phantom at 90 kVp and 110 mAs, ~180 slices, with a 3-mm thickness and zero gaps in the transverse plane

using a large-bore (70 cm) multi-slice CT scanner (Neusoft Company, China).

MRI acquisitions were performed using a 60-cm bore MAGNETOM® Symphony Syngo 1.5 T (Siemens Company, Germany). For the evaluation and correction of geometric distortion, T2 weighted HASTE sequence, which is a clinical conventional protocol of pelvic region, was acquired using a 2D vendor correction algorithm for the MRI planning of the pelvic region. Parameters of T2 HASTE sequence for the assessment of image distortion are summarized in Table 1.

CT and MRI Image registrations

Images registration plays an important role in the process of treating patients in the radiation therapy department at various stages of treatment design, image-guided therapy, assessment of time series images, and the follow-up of patients [28].

There are several methods of rigid, affine, and deformable image registration that can be used based on the type of image and the purpose of the study. In rigid registration, six degrees of freedom of translations and rotations have been considered and all distances are preserved. This kind of registration can be suitable for image registration of one modality without any deformable in structures [28]. Another method of registration is affine registration which has added scaling and shearing parameters to rigid registration [29]. More degrees of freedom have been provided in deformable registration that every voxel of the image has a special transformation matrix. In the registration of time series images, multimodality images, and geometric distortion correction of images, deformable registrations methods show better performance.

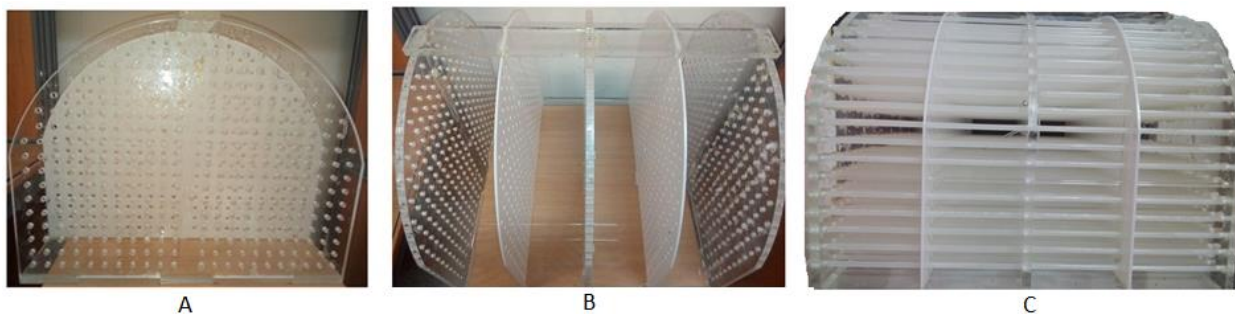


Figure 2. A) 325 holes in Perspex sheets, B) arrangement of 6 Perspex sheets, C) phantom filled with pipes.

Table 1. Parameters of the T2_HASTE sequence

protocol	Half-Fourier-Acquired Single-shot Turbo spin Echo (HASTE)
Scanning Sequence	SE (Spin Echo)
MR Acquisition Type	2D
Slice Thickness	3 mm
Spaces between Slices	0 mm
Repetition Time	531 ms
Echo Time	78 ms
Spacing Between Slices	3 mm
Pixel Band Width	475 Hz/pixel
Flip Angle	150

The B-spline deformable registration method is a kind of deformable registration algorithm that is suitable for deriving transforms between image volumes exhibiting complex local variations such as geometric distortion [30].

In this study for the evaluation of distortion, rigid registration, and for the correction of geometric distortion B-spline deformable correction method have used.

Evaluation and correction of geometric distortion in MRI images of the phantom

In the first stage, CT and MRI images of the phantom were registered by the rigid registration or linear registration in the Transform Module of the 3D slicer software (version 4.8) [31]. Manual rigid

registration of CT and MRI images of the phantom is done by using the markers near the isocenter so the distortion is minimized.

For the quantitative assessment of geometric distortion, the position of markers was delineated manually using the Markups Module of the 3D slicer software [31] and filed with .fcsv format (a list of data separated by commas) that contains coordinates of markers to be imported to MATLAB software (ver. 2014) [32]. In MATLAB software, two separate matrices were defined for the coordinates of the points. Each matrix contains the spatial coordinates of the markers (X, Y, and Z) in CT and MRI images that were considered as reference and displaced points.

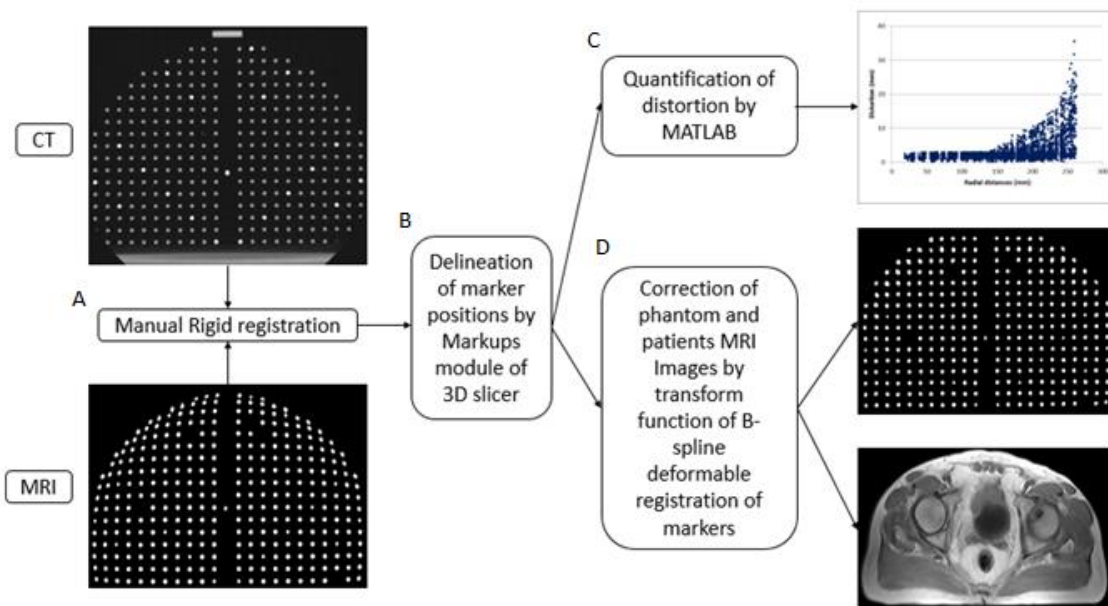


Figure 3. Stages of evaluation and correction of geometric distortion ; A: CT-MR registration, B: Delineation of marker positions in CT and MR images, C: quantification of geometrical distortion, D: correction of geometrical distortion

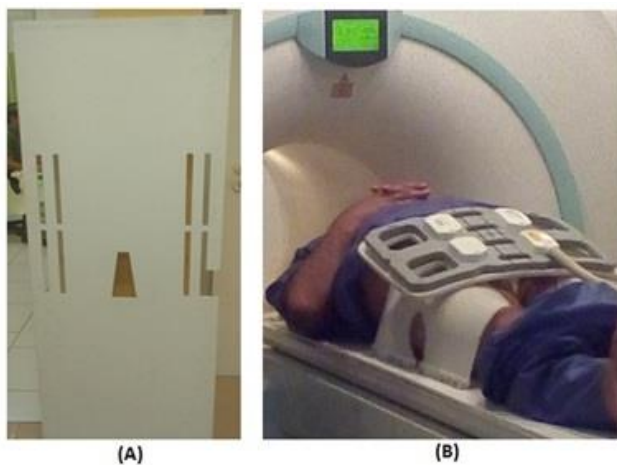


Figure 4. (A) Flat overlay table, and (B) patient positioning before MR imaging

The difference of markers was calculated based on formulas for calculation of the distance and was reported as the amount of MRI image geometric distortion.

We used MATLAB software for the MRI image's geometrical distortion quantification and representation. For the purpose of distortion correction, .fcsv files containing CT and MR markers were imported to the scatter transform module of the 3D slicer as fix and moving points, respectively. B-spline deformable transform function obtained from the scatter transform module [31] was applied to the MRI image of the phantom to correct geometric distortion.

The stages of evaluation and MRI images geometric distortion correction are shown in Figure 3.

Flowchart of patient's MRI images geometrical distortion evaluation and correction

For this study, we recruited ten patients with pelvic cancer diagnostic. We included all prostate, rectum, bladder, and uterus cancer cases. All CT and MRI images (HASTE) were acquired. The patients were all scanned at the same position with a flat layer table and thermoplastic mask (Figure 4). Both CT and MRI images were taken with the technique of deep breathing and breath-holding, during imaging. This study had no effect on the radiotherapy procedure of the patients (ethical approval ID: IR.MUMS.MEDICAL.REC.1397.305).

We rigidly registered of CT and MR images using 3D slicer software (version 4.8.1) according to bone landmarks. The correction function was applied to MRI images using the transform module of 3D slicer software. Finally, we compared the lateral (LAT) and anterior-posterior (AP) diameters of CT, non-corrected MRI, and corrected MRI images for analysis. Similarity evaluation of images by Dice similarity coefficient between the volumes of CT, non-corrected MRI, and corrected MRI images have been done by using of Dice Computation module of 3D slicer software.

Results

Phantom Study

According to the quantitative results of geometric distortion, at radial distances of < 13 cm (FOVs < 25 cm) the amount of distortion is less than 2 mm, but at radial distances of > 13 cm, the distortion is escalated, reaching about 3.5 cm at radial distances of more than 25 cm. The

amount of geometric distortion relative to the radial distance is shown in Figure 5.

The transform function could reduce the geometric distortion of the image to a maximum of 2 mm at all points of the MR image. The non-corrected and corrected slices of -15, -5, +5, and +15 cm are shown in Figure 6.

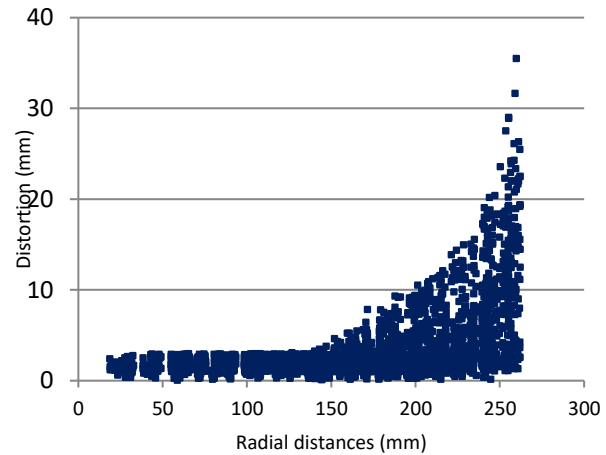


Figure 5. The displacement of markers in MR images according to the radial distance from the isocenter point

Patient Study

Then vector representation of correction functions acquired based on phantom data, were fused and overlaid on the patient's data for better MRI image geometrical distortion. The non-corrected MRI image of one patient at the LAT and AP diameters in various slices of -10, -5, 0, 5, 10 and 15 cm is shown in Figure 7. The transform vectors shown in Figure 7 reveal the points with distortions of more than 2 mm. distortion evaluations according to MRI images of patients, showed that for LAT and AP diameters less than 38 cm and 25 cm, respectively, the amount of distortion was less than 2 mm that is acceptable for radiotherapy applications [17]. The results suggest that the MRI image of patients with a LAT diameter of more than 38 cm need to be corrected for the geometric distortion.

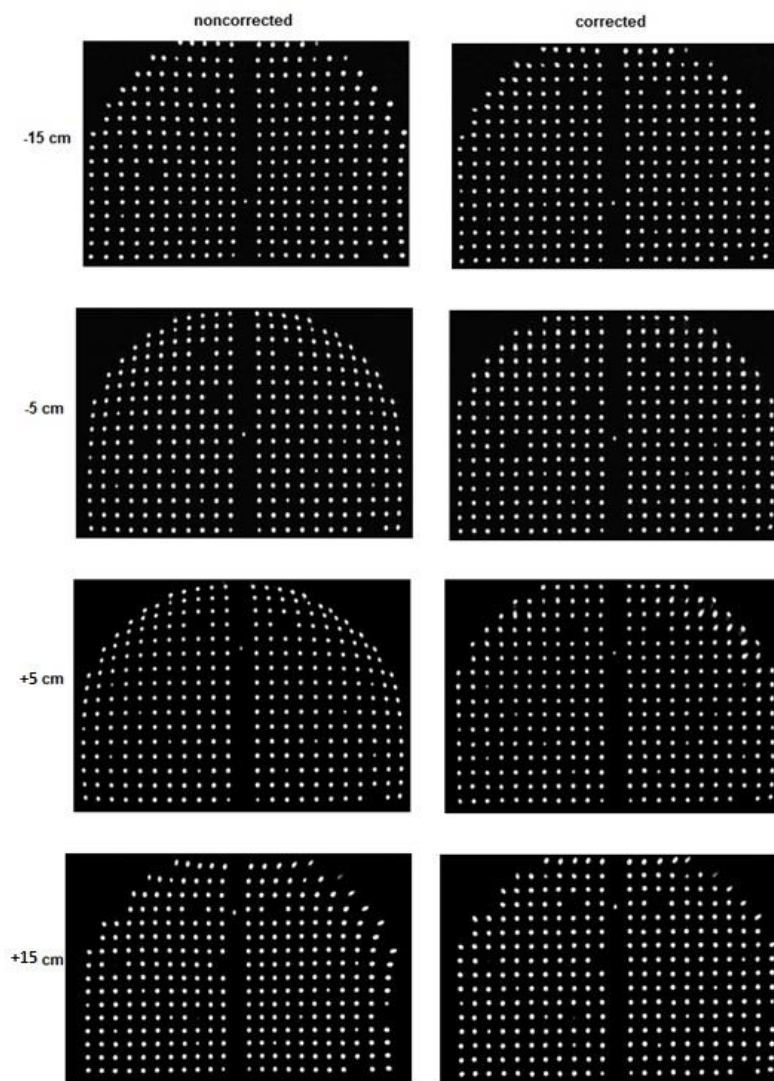


Figure 6. Non-corrected and corrected MR images in different slices of -15, -5, 5, and 15 cm; left and right columns show non-corrected and corrected images, respectively.

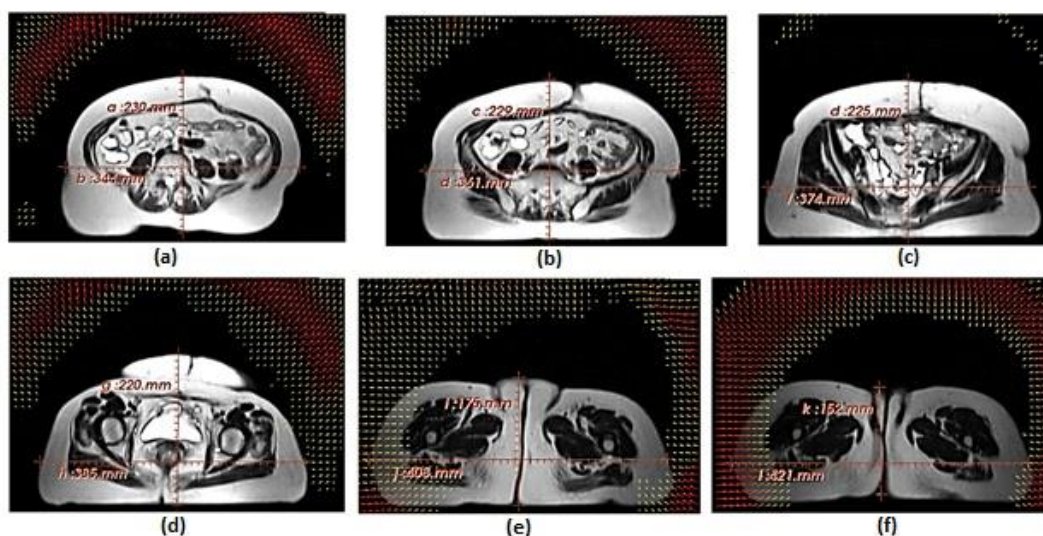


Figure 7. LAT and AP diameters of a patient in various slices of (a) -10, (b) -5, (c) 0, (d) 5, (e) 10 and (d) 15 cm in combination with vectors of MR correction function.

Table 2. Maximum LAT and AP diameters of patients

patient	Maximum LAT separation (cm)	Maximum AP separation (cm)
1	36.96	20.60
2	35.40	19.20
3	33.10	16.13
4	33.42	18.35
5	35.64	21.90
6	37.67	15.94
7	37.81	21.23
8	40.8	23.45
9	37.86	19.57
10	41.63	24.26

Table 3. Maximum LAT separation, amount of image distortion and DSC of two patients in CT, non- corrected and corrected MR images

patient	Maximum LAT separation in CT image (cm)	Maximum LAT separation in non-corrected MR image (cm)	Maximum LAT separations in corrected MR image (cm)	Amount of image distortion in LAT direction (cm)	DSC of CT and non-corrected MR	DSC of CT and corrected MR
8	40.80	42.14	40.53	1.34	0.88	0.97
10	41.63	43.21	41.85	1.58	0.89	0.98

Based on the maximum LAT and AP diameters in CT images reported in Table 2, just two patients had LAT diameter more than 38 cm that should be corrected. The results of correction function applying to their MRI images have been shown in table 3 by maximum separations, amount of distortion and dice similarity coefficient (DSC) for CT, non-corrected MR, and corrected MR images.

Discussion

One of the critical quality control (QC) procedures for MRI-based radiotherapy planning is checking the MRI images' geometrical distortion. There are machine and patient-specific sources of MRI image geometrical distortion. In this study, we construct our large in-house field of view phantom and study its feasibility to map out MRI images' geometrical distortion using our simulation MRI pulse sequence. We also extend the application and hypothesis that maybe this phantom can help us identify the gross distortion region for body radiotherapy patients.

The large FOV phantom consisting of pipes instead of markers allows slice-by-slice assessment of distortion within thin slices with no gap to improve the precision. Although the phantom is unable to reveal distortions in the Z direction, the effect of distortions in X and Y directions on external contour or skin contour is more than the Z direction in the dosimetry calculation stage of radiotherapy [17].

The results exhibit that the correction function captured by the phantom is capable to correct MRI images of the patients with acceptable precision for common radiotherapy applications. But, the special techniques of SRS, SRT, and IMRT need more accurate geometrical precision and the evaluation of patient-related and system-related Geometrical distortion in 3D view must be done. It should be mentioned that the accurate internal and external contour of the MRI protocol for MR-based radiotherapy is highly important

for dosimetry calculation precision. For the contouring of internal organs, the imaging of different protocols with small FOVs could be used for greater geometric precision. It means a combination of several protocols can be used for organ contouring and pseudo-CT construction [10, 27].

There are four main reasons for choosing the HASTE protocol for evaluation and correction of the geometric distortion, in this study.

1. T2w sequences are usually preferred for pelvic region imaging and this also applies to external radiotherapy and brachytherapy planning. T2w HASTE sequence is a clinical conventional protocol for pelvic region imaging.
2. In the following geometric distortion evaluation and correction of the images, pseudo-CT construction, and dosimetric comparison have been done. In the construction of the pseudo-CT, the HASTE images have been used. So geometric distortion has been corrected on this sequence.
3. Examination of the 4 protocols of TSE, TIRM, HASTE, and FLASH in our previous work, showed that the amount of geometric error in this sequence is less than in the other sequences. This can be related to the received bandwidth, which is more than 440 Hz/pixel in the HASTE sequence. Different studies show that increasing BW is a critical factor in the reduction of geometric distortions [33]. several studies suggest the BW is at least 440 Hz/pixel for MR-based planning, but the increase of BW decrease the SNR, therefore, a trade-off between SNR and geometric fidelity is necessary [34].
4. HASTE is a fast sequence with time imaging of about 16 s, therefore the patients can perform breathe holding technique in the imaging time.

Evaluation of MR geometrical distortion have been reported by different 2D and 3D phantoms. Polyurethane foam plates with polyethylene markers have been used for image distortion evaluation of three MRI scanners by Price et al. [19]. They reported distortions of less than 1 mm for the FOV < 15 cm, but at larger distances, the amount of distortion is increased to 6 mm. In the other study by Walker et al., the FLUKE biomedical phantom (an acrylic phantom with 397 holes containing saline as the signal creator) has been used to assess the distortion of four imaging protocols in four clinical MRI scanners [20]. Based on the results of their study, the distortion is specific to each scanner and protocol; moreover, it is dependent on the receiver bandwidth (rBW). The MRI image distortion evaluation by Perspex cubic phantom containing grid plastic layers revealed that the distortion could reach 25 mm. Also, the distortion correction by the piecewise interpolation method could reduce it to about 0.8 mm. Due to the complicated spatial characteristics of MRI geometric distortion, non-linear functions of piecewise interpolation can provide suitable flexibility and smoothness to represent the local features of the geometric distortion [11, 21].

Torfeh et al. utilized a larger FOV phantom with foam layers and ellipsoidal markers for the assessment of 2D and 3D vendor correction algorithms. The evaluation of several 2D and 3D imaging sequences exhibited that the 3D vendor correction program was able to reduce distortion to 1.9 mm [22]. In the other study by Walker et al., the MRI imaging of plastic layers containing vitamin E has been performed using the static and moving tables of the MRI scanner. According to the results, the distortion reduced in moving table protocols and the lowest geometric distortion has been reported at a table speed of 1.1 mm/s [13].

The results of geometric distortion assessment suggest that 2D geometrical distortion correction algorithms of the MRI system yield desirable geometric precision for FOVs < 25 cm (distortion < 2 mm). This geometrical precision of imaging in FOVs < 25 cm is suitable for the head, but for the regions of the thorax, abdomen, and pelvic, the geometric distortion can be reached 3.5 cm, which is not acceptable for the MRI-based treatment planning [35, 36]. The reported MRI image's radial geometric distortion is in agreement with other studies, which are suitable for head and neck radiotherapy planning [37-39].

The pattern of geometrical distortion is changing along the slices. The B-spline deformable registration of points with the scatter transform of the 3D slicer and the deformable map can correct the geometric distortion of MR images in all slices (Figure 6.). For correction of MR geometric distortion, the displacement vector mappings of B-spline deformable registration method have been applied on MR images by using of the transform module of 3D slicer software. By this correction method, the geometrical precision reaches 2 mm, which is acceptable for common radiotherapy

applications [35, 36]. It is also in agreement with the correction method adopted by Wang et al. and Price et al., who reported a maximum distortion of 0.6 mm and 9.5 mm after correction, respectively [15, 22, 23].

The evaluation of geometric distortion based on the MRI images of ten patients showed that just the patients with more than 38 cm and 25 cm LAT and AP diameters need to be corrected in terms of geometric distortion. In a similar study by Chen et al. For the dosimetry accuracy of MRI-based treatment planning, patients with maximum LAT dimensions of 38 cm have been selected for the study. They showed that the geometric distortion correction software of the MR system worked well for patient sizes less than 38 cm with distortion errors less than 7 mm [40]. The low difference in geometric distortion between our study and the result of Chen et al. can be associated with the different MR imaging protocols.

In the first step toward MRI planning, we have designed a large field of view phantom that has continuous markers in the Z direction, and in every Z amount we could have the distortion in X and Y directions, but there are two major limitations in our work.

- we do not have any information about the distortion in the Z direction that can be solved by using a more suitable marker-based phantom. By a large FOV marker-based phantom, the geometric distortion of MRI images can be evaluated and corrected accurately in 3 directions of X, Y, and Z, especially in radiotherapy techniques of SRS, SRT, and IMRT.
- The position of markers in CT and MRI images was delineated manually which is time-consuming. Automatic methods of marker delineation are intended for our future study.

Quality evaluation of MRI images by using patient positioning instruments and the precision of pseudo-CT construction according to corrected MRI images have been evaluated in our future work. Using another deformable registration package, like open source toolkit Advanced Normalization Tools (ANTs) [41] to evaluate the effectiveness and compare it with the results of this study is one of the suggestions.

Conclusion

A large FOV house-made phantom and the evaluation and correction method presented in this study can provide deeper insights into the system-related geometrical distortion. The geometric distortion analysis of MR images show that the geometric precision is within the acceptable range of 2 mm for the common radiotherapy application in FOVs < 25 cm and additional correction is required for larger FOVs.

The amount and pattern of geometric distortion is dependent to slice location. Using of scatter transform module of 3D slicer software by the B-spline deformable registration method can correct the geometric distortion of phantom MR images up to geometric precision of 2 mm that it is acceptable for

common radiotherapy applications. The evaluation and correction of ten patient's MR images exhibit that for patients with the separation more than 38 cm, it is essential to use geometric distortion correction for treatment planning radiotherapy applications.

Acknowledgment

This paper was extracted from a PhD thesis of Medical Physics. The authors would like to thank the Research Deputy of MUMS for financial support of this project, numbered (961527).

References

- Paulus DH, Oehmigen M, Grueneisen J, Umutlu L, Quick HH. Whole-body hybrid imaging concept for the integration of PET/MR into radiation therapy treatment planning. *Physics in Medicine & Biology*. 2016 Apr 7;61(9):3504.
- Schmidt MA, Payne GS. Radiotherapy planning using MRI. *Physics in Medicine & Biology*. 2015 Oct 28;60(22):R323.
- Metcalfe P, Liney GP, Holloway L, Walker A, Barton M, Delaney GP, Vinod S, Tome W. The potential for an enhanced role for MRI in radiation-therapy treatment planning. *Technology in cancer research & treatment*. 2013 Oct;12(5):429-46.
- Laruelo A. Integration of magnetic resonance spectroscopic imaging into the radiotherapy treatment planning (Doctoral dissertation, Université Paul Sabatier-Toulouse III).
- Dai YL, King AD. State of the art MRI in head and neck cancer. *Clinical radiology*. 2018 Jan 1;73(1):45-59.
- Leung D, Han X, Mikkelsen T, Nabors LB. Role of MRI in primary brain tumor evaluation. *Journal of the National Comprehensive Cancer Network*. 2014 Nov 1;12(11):1561-8.
- Price RG, Kim JP, Zheng W, Chetty IJ, Glide-Hurst C. Image guided radiation therapy using synthetic computed tomography images in brain cancer. *International Journal of Radiation Oncology* Biology* Physics*. 2016 Jul 15;95(4):1281-9.
- Balter J, Cao Y, Wang H, Huang K, Hsu SH, Requardt M, Shea SM. Optimizing MRI for radiation oncology: initial investigations. *MAGNETOM Flash*. 2013;45.
- Wang H, Du K, Qu J, Chandarana H, Das IJ. Dosimetric evaluation of magnetic resonance-generated synthetic CT for radiation treatment of rectal cancer. *PLoS One*. 2018 Jan 5;13(1):e0190883.
- Tyagi N, Fontenla S, Zelefsky M, Chong-Ton M, Ostergren K, Shah N, Warner L, Kadbi M, Mechalakos J, Hunt M. Clinical workflow for MR-only simulation and planning in prostate. *Radiation Oncology*. 2017 Dec;12(1):1-2.
- Wang C, Chao M, Lee L, Xing L. MRI-based treatment planning with electron density information mapped from CT images: a preliminary study. *Technology in cancer research & treatment*. 2008 Oct;7(5):341-7.
- Aldosary G, Szanto J, Holmes O, Lavigne B, Althobaity W, Sheikh A, Footitt C, Vandervoort E. Geometric inaccuracy and co-registration errors for CT, DynaCT and MRI images used in robotic stereotactic radiosurgery treatment planning. *Physica Medica*. 2020 Jan 1;69:212-22.
- Walker A, Liney G, Holloway L, Dowling J, Rivest-Henault D, Metcalfe P. Continuous table acquisition MRI for radiotherapy treatment planning: distortion assessment with a new extended 3D volumetric phantom. *Medical physics*. 2015 Apr;42(4):1982-91.
- Adjeiwaah M, Bylund M, Lundman JA, Karlsson CT, Jonsson JH, Nyholm T. Quantifying the effect of 3T magnetic resonance imaging residual system distortions and patient-induced susceptibility distortions on radiation therapy treatment planning for prostate cancer. *International Journal of Radiation Oncology* Biology* Physics*. 2018 Feb 1;100(2):317-24.
- Price RG, Kadbi M, Kim J, Balter J, Chetty IJ, Glide-Hurst CK. Characterization and correction of gradient nonlinearity induced distortion on a 1.0 T open bore MR-SIM. *Medical physics*. 2015 Oct;42(10):5955-60.
- Weygand J, Fuller CD, Ibbott GS, Mohamed AS, Ding Y, Yang J, Hwang KP, Wang J. Spatial precision in magnetic resonance imaging-guided radiation therapy: the role of geometric distortion. *International Journal of Radiation Oncology* Biology* Physics*. 2016 Jul 15;95(4):1304-16.
- Paulson ES, Crijns SP, Keller BM, Wang J, Schmidt MA, Coutts G, van der Heide UA. Consensus opinion on MRI simulation for external beam radiation treatment planning. *Radiation Oncology*. 2016 Nov 1;12(12):187-92.
- Lundman JA, Johansson A, Olofsson J, Axelsson J, Larsson A, Nyholm T. Effect of gradient field nonlinearity distortions in MRI-based attenuation maps for PET reconstruction. *Physica Medica*. 2017 Mar 1;35:1-6.
- Price RG, Knight RA, Hwang KP, Bayram E, Nejad-Davarani SP, Glide-Hurst CK. Optimization of a novel large field of view distortion phantom for MR-only treatment planning. *Journal of applied clinical medical physics*. 2017 Jul;18(4):51-61.
- Walker A, Liney G, Metcalfe P, Holloway L. MRI distortion: considerations for MRI based radiotherapy treatment planning. *Australasian physical & engineering sciences in medicine*. 2014 Mar;37(1):103-13.
- Wang D, Strugnell W, Cowin G, Doddrell DM, Slaughter R. Geometric distortion in clinical MRI systems: Part I: evaluation using a 3D phantom. *Magnetic resonance imaging*. 2004 Nov 1;22(9):1211-21.
- Torfeh T, Hammoud R, Perkins G, McGarry M, Aouadi S, Celik A, Hwang KP, Stancanello J, Petric P, Al-Hammadi N. Characterization of 3D geometric distortion of magnetic resonance imaging scanners commissioned for radiation therapy planning. *Magnetic resonance imaging*. 2016 Jun 1;34(5):645-53.
- Wang D, Doddrell DM, Cowin G. A novel phantom and method for comprehensive 3-dimensional measurement and correction of geometric distortion in magnetic resonance imaging. *Magnetic resonance imaging*. 2004 May 1;22(4):529-42.
- Wang D, Strugnell W, Cowin G, Doddrell DM, Slaughter R. Geometric distortion in clinical MRI systems: Part II: correction using a 3D phantom.

- Magnetic resonance imaging. 2004 Nov 1;22(9):1223-32..
25. Damyanovich AZ, Rieker M, Zhang B, Bissonnette JP, Jaffray DA. Design and implementation of a 3D-MR/CT geometric image distortion phantom/analysis system for stereotactic radiosurgery. *Physics in Medicine & Biology*. 2018 Mar 27;63(7):075010.
 26. Rostami A, Naseri S, Momenzhad M, Zare H, Anvari K, Badkhor HS. Geometric distortion evaluation of magnetic resonance images by a new large field of view phantom for magnetic resonance based radiotherapy purposes. *International Journal of Radiation Research*. 2020 Oct 1;18(4):733-42.
 27. Tyagi N, Fontenla S, Zhang J, Cloutier M, Kadbi M, Mechalakos J, Zelefsky M, Deasy J, Hunt M. Dosimetric and workflow evaluation of first commercial synthetic CT software for clinical use in pelvis. *Physics in Medicine & Biology*. 2017 Mar 17;62(8):2961.
 28. Wyawahare MV, Patil PM, Abhyankar HK. Image registration techniques: an overview. *International Journal of Signal Processing, Image Processing and Pattern Recognition*. 2009 Sep;2(3):11-28
 29. Hill DL, Batchelor PG, Holden M, Hawkes DJ. Medical image registration. *Physics in medicine & biology*. 2001 Mar 1;46(3):R1.
 30. Rueckert D, Sonoda LI, Hayes C, Hill DL, Leach MO, Hawkes DJ. Nonrigid registration using free-form deformations: application to breast MR images. *IEEE transactions on medical imaging*. 1999 Aug;18(8):712-21.
 31. Fedorov A., Beichel R., Kalpathy-Cramer J., Finet J., Fillion-Robin J-C., Pujol S., Bauer C., Jennings D., Fennessy F.M., Sonka M., Buatti J., Aylward S.R., Miller J.V., Pieper S., Kikinis R. 3D Slicer as an Image Computing Platform for the Quantitative Imaging Network. *Magn Reson Imaging*. 2012 Nov;30(9):1323-41.
 32. MATLAB 2018a, The MathWorks, Inc., Natick, Massachusetts, United States.
 33. Vanel D. MRI of bone metastases: the choice of the sequence. *Cancer Imaging*. 2004;4(1):30.
 34. Koivula L. Magnetic resonance imaging-based radiation therapy treatment planning.
 35. Stanescu T, Hans-Sonke J, Stavrev P, Fallone BG. 3T MR-based treatment planning for radiotherapy of brain lesions. *Radiology and Oncology*. 2006 Jun 1;40(2).
 36. Stanescu T, Jans HS, Pervez N, Stavrev P, Fallone BG. A study on the magnetic resonance imaging (MRI)-based radiation treatment planning of intracranial lesions. *Physics in Medicine & Biology*. 2008 Jun 17;53(13):3579.
 37. Andreasen D, Van Leemput K, Hansen RH, Andersen JA, Edmund JM. Patch-based generation of a pseudo CT from conventional MRI sequences for MRI-only radiotherapy of the brain. *Medical physics*. 2015 Apr;42(4):1596-605.
 38. Chen L, Price RA, Nguyen TB, Wang L, Li JS, Qin L, Ding M, Palacio E, Ma CM, Pollack A. Dosimetric evaluation of MRI-based treatment planning for prostate cancer. *Physics in medicine & biology*. 2004 Oct 29;49(22):5157.
 39. Jonsson JH, Akhtari MM, Karlsson MG, Johansson A, Asklund T, Nyholm T. Accuracy of inverse treatment planning on substitute CT images derived from MR data for brain lesions. *Radiat Oncol*. 2015;10(1):13.
 40. Chen L, Price R, Wang L, Li J, Qin L, Mcneelely Sh, et al. MRI-BASED TREATMENT PLANNING FOR RADIOTHERAPY: DOSIMETRIC VERIFICATION FOR PROSTATE IMRT. *Int J Radiat Oncol Biol Phys*. 2004.60(2);636-647.
 41. Avants BB, Tustison N, Song G. Advanced normalization tools (ANTs). *Insight j*. 2009 Jun 4;2(365):1-35.